Laminar mixed convection in air between horizontal heated rotating cylinders

Samy M. El-Sherbiny
Mechanical Eng. Dept., Faculty of Eng., Alexandria University, Alexandria, Egypt

Laminar mixed convection in air layers (Pr=0.71) between two concentric horizontal cylinders at different uniform temperatures is numerically investigated. The forced flow is induced by the rotation of the inner heated cylinder or the outer cooled one with constant angular velocity. The study covered various combinations of Ra, Re and radius ratio, RR in the range of $10^2 \le Ra \le 10^7$, $0 \le Re \le 3000$ and $1.20 \le RR \le 10$. Maps of the streamlines and isotherms are developed to explain the flow characteristics and heat transfer. The effects of the different parameters on the average Nu are investigated.

يقدم البحث دراسة عددية لأنتقال الحرارة بالحمل الحر والقسرى فى طبقات من الهواء محصورة بين أسطوانتين أفقيتين ومتحدتى المحور. الحمل القسري ينتج من دوران الأسطوانة الداخلية الساخنة أو الأسطوانة الخارجية الباردة. وقد شملت الدراسة مدى واسع من أرقام رالى من ١٠^{٢} الى ١٠^{٧} ورينولدز من صفر الى ٣٠٠٠ وذلك عند نسب مختلفة من أقطار الأسطوانتين من ١,٢ الى ١٠ . وقدم البحث دراسة لتأثير النسبة بين قطرى الأسطوانتين على عملية أنتقال الحرارة بالحمل الحر. وعرض البحث أشكال توزيع خطوط السريان ودرجات الحرارة لحالات متنوعة فى مدى الدراسة لشرح خواص السريان وأنتقال الحرارة. كما قدم جميع النتائج العددية لرقم نوسلت المتوسط وتأثير كل من عوامل الدراسة المختلفة على عملية أنتقال الحرارة.

Keywords: Mixed convection, Horizontal annulus, Numerical analysis, Rotating cylinders

1. Introduction

The problem of heat transfer and flow characteristics in the annulus between two concentric cylinders was given a considerable attention due to its theoretical interest and wide engineering applications. This includes thermal energy storage systems, solar collector receivers, cooling of electronic components, cooling system in nuclear reactors, rotating machinery and transmission cables.

A comprehensive review in the case of natural convection in the horizontal annulus was presented by Kuehn and Goldstein [1]. Powe et al. [2,3] and Rao et al. [4] investigated the flow patterns and found that the free convective flow of a high Pr fluid ($Pr \ge 1$) can be classified into four basic types: a steady two-dimensional flow with two crescent-shaped eddies, a two-dimensional oscillatory flow , a three-dimensional spiral flow and a two-dimensional multicellular flow. Recently, Yoo [5] investigated the existence of dual steady solutions for a fluid of Pr = 0. 7. Effect of annulus eccentricity on the overall heat transfer was investigated by [6, 7].

Mixed Convection in rotating systems has been investigated for the flows in vertical cylindrical annuli [8-10] and within a horizontal annulus with a heated rotating inner cylinder [11-14]. In mixed convection, the forced flow can aid or oppose the buoyancy-induced flow. However, in the horizontal annulus, both effects exist. The effect of rotating the inner cylinder for a concentric annulus was first studied by Taylor [15]. He showed that, above a critical speed of rotation, the laminar Couette flow breaks down into a flow consisting of pairs of three-dimensional ring-shaped vortices spaced regularly along the length of the cylinders (Taylor vortices).In this case, the torque on the outer cylinder and the heat transfer across the gap are dramatically increased. Bjorklund and Kays [16] presented experimental heat transfer data for different values of RR in the range $1.05 \le RR \le 1.25$ and for several combinations of outer to inner cylinder speed. The heat transfer performance indicates three regimes of flow; the first is at low peripheral velocities in which laminar flow and heat transfer by conduction prevail. The second is at cylinder speeds above a theoretically predictable value in which vortex flow oc-

curs and is the controlling mechanism. The third is at still higher speeds, where a distorted type of vortex motion may be present. When the inner cylinder or both of the inner and outer cylinders are rotating at constant angular velocity, the centrifugal effects created by the rotating cylinder can lead to three-dimensional flows with Taylor vortices [17]. In this case, linear stability theory shows that the flow is not always stable for all values of the angular velocity. Fusegi et al. [11] and Lee [12,14] limited the calculations to a range of parameters that would exclude this possibility. Fusegi et al. [11] performed numerical analysis for two-dimensional mixed convection in a horizontal annulus with a heated rotating inner cylinder at $RR = 2.6$, $Pr = 0.72$, $10^2 \le Ra \le 10^5$ and $1 \le Gr/Re^2 \le \infty$ (pure natural convection). The numerical calculations carried out by Lee [14] covered the range $3.9\times10^3 \le Ra \le 3.9\times10^6$, $0 \le Re \le 2800$ at $Pr = 0.7$ and $RR = 2.6$. The results showed that the mean Nusselt number increases with *Ra*. For a fixed *Ra*, when the inner cylinder is made to rotate, the mean Nu decreased with *Re*.

On the contrary, the Couette flow between two horizontal concentric cylinders, with fixed inner cylinder and rotating outer one with constant angular velocity, proved to be stable for all values of the angular velocity. There is, of course, a possibility of three-dimensional flows for nonlinear disturbances at sufficiently high *Ra* and *Re*. Yoo [18] found that the flow patterns can be categorized into three basic types according to the number of eddies: two-eddy, one-eddy and no-eddy flows. A map of the three flow regimes for steady-state was constructed on the *Ra-Re* plane.

In the present numerical study, the two-dimensional mixed convection in a horizontal annulus is investigated. The inner cylinder is hotter than the outer one and the forced flow is induced by the rotation of either the inner cylinder or the outer one with constant angular velocity. The effects of the forced flow on the characteristics of heat transfer and fluid flow are investigated. Numerical calculations are made for various combinations of Ra, *Re* and *RR* in the range of $10^2 \le Ra \le 10^7$, $0 \le Re \le 3000$ and $1.20 \le RR \le 10$ with $Pr = 0.71$ (air).

2. Mathematical analysis

The geometry of the two-dimensional problem and the cylindrical coordinate system (R, φ) are shown in fig. 1. Air is contained between two infinite horizontal concentric cylinders at different uniform temperatures. The inner cylinder is heated to T_h and the outer one is cooled to T_c. The density change in the fluid is neglected everywhere except in the buoyancy term and all other fluid physical properties are assumed constant (Boussinesq approximation). Viscous dissipation is also neglected.

2.1. Governing equations

The steady-state dimensionless equations governing conservation of mass, momentum and energy are given as:

$$\frac{\partial V_r}{\partial R} + \frac{V_r}{R} + \frac{\partial V_\phi}{R\partial \phi} = 0 , \tag{1}$$

$$\left(V_r \frac{\partial V_r}{\partial R} + V_\phi \frac{\partial V_r}{R\partial \phi} - \frac{V_\phi^2}{R} \right) = -\frac{\partial P_d}{\partial R} - \frac{Ra}{8\,Pr}\theta \cos\phi +$$

$$\left(\frac{\partial^2 V_r}{\partial R^2} + \frac{1}{R}\frac{\partial V_r}{\partial R} - \frac{V_r}{R^2} + \frac{\partial^2 V_r}{R^2 \partial \phi^2} - \frac{2}{R^2}\frac{\partial V_\phi}{\partial \phi} \right), \tag{2}$$

$$\left(V_r \frac{\partial V_\phi}{\partial R} + V_\phi \frac{\partial V_\phi}{R\partial \phi} + \frac{V_r V_\phi}{R} \right) = -\frac{\partial P_d}{R\partial \phi} + \frac{Ra}{8\,Pr}\theta \sin\phi +$$

$$\left(\frac{\partial^2 V_\phi}{\partial R^2} + \frac{1}{R}\frac{\partial V_\phi}{\partial R} - \frac{V_\phi}{R^2} + \frac{\partial^2 V_\phi}{R^2 \partial \phi^2} + \frac{2}{R^2}\frac{\partial V_r}{\partial \phi} \right), \tag{3}$$

$$\left(V_r \frac{\partial \theta}{\partial R} + V_\phi \frac{\partial \theta}{R\partial \phi} \right) = \frac{1}{Pr}\left[\frac{1}{R}\frac{\partial}{\partial R}\left(R\frac{\partial \theta}{\partial R} \right) + \frac{\partial^2 \theta}{R^2 \partial \phi^2} \right]. \tag{4}$$

The following dimensionless variables are used:

$$V_r = \frac{v_r}{(\nu/a)}, \quad V_\phi = \frac{v_\phi}{(\nu/a)}, \quad R = \frac{r}{a}, \quad \theta = \left(\frac{T - T_c}{T_h - T_c} \right),$$

$$P_d = \frac{\mathrm{p_d}}{\rho(\nu/a)^2}, \quad \mathrm{Pr} = \frac{Cp\mu}{k},$$

$$Ra = \frac{\beta\, g (T_h - T_c)(2a)^3}{\nu\alpha}. \tag{5}$$

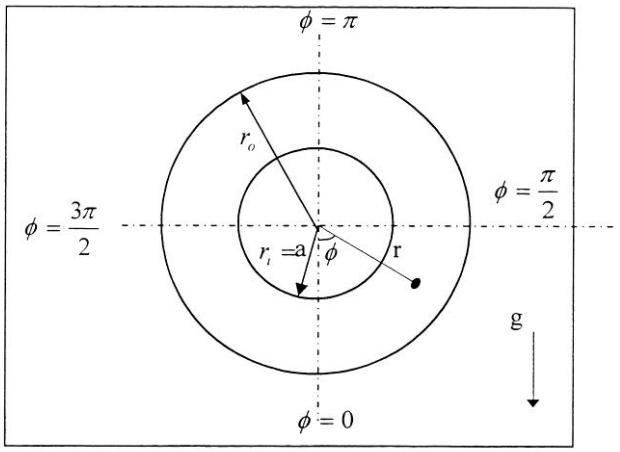

Fig. 1. Problem configuration.

Three different cases are investigated and their boundary conditions are given as:

Case (a) free convection:
at $R = 1$ and $0 \le \varphi \le 2\pi$, $Vr = 0$, $V_\varphi = 0$, $\theta = 1$,
at $R = RR$ and $0 \le \varphi \le 2\pi$, $V_r = 0$, $V_\varphi = 0$, $\theta = 0$

Case (b) Rotating inner cylinder (counter clockwise):
at R=1 and $0 \le \varphi \le 2\pi$, Vr =0, V_φ =0.5 Re, $\theta = 1$
at $R = RR$ and $0 \le \varphi \le 2\pi$, $V_r = 0$, $V_\varphi = 0$, $\theta = 0$

Case (c) Rotating outer cylinder (counter clockwise):
at $R = 1$ and $0 \le \varphi \le 2\pi$, $Vr = 0$, $V_\varphi = 0$, $\theta = 1$
at R=RR and $0 \le \varphi \le 2\pi$,, V_r =0, V_φ=0.5 Re, $\theta = 0$.

Where, *Re* is the Reynolds number defined as $Re = 2\ \omega\ a^2/\nu$.

2.2. Nusselt number calculations

The local Nusselt number, Nu_ϕ on the inner hot cylinder is defined as:

$$Nu_\phi = \frac{h_\phi(2a)}{k} = -2\frac{\partial\theta}{\partial R}\Big|_{R=1}, \qquad (6)$$

and the average Nusselt number, *Nu* over the inner cylinder is given as:

$$Nu = \frac{h(2a)}{k} = \frac{-1}{\pi}\int_0^{2\pi}\frac{\partial\theta}{\partial R}d\phi\ . \qquad (7)$$

2.3. Numerical solution

The governing eqs. (1-4) with their boundary conditions for each of the three cases are solved using the finite difference technique developed by Patankar [19]. The discretized equations used central differencing in space and were solved by Gauss-Seidel elimination method. A line by line procedure is used in the iterations. The continuity and momentum equations are first solved simultaneously and then the energy equation. A converged solution is considered when the change in the average Nusselt number over 100 iterations is less than 0.01 % of its value. The number of iterations used to get a converged solution ranged from 1500 to 2500 iterations. The ($r\times\varphi$) grid mesh used in the numerical solution is (50×90). In the azimuthal direction, a uniform grid is used but in the radial direction, a non-uniform grid is used. The nodes are denser near the cylinder walls to sufficiently resolve the thin boundary layer near the cylinders.

3. Results and discussion

To check the numerical method, the problem of pure conduction and that of pure natural convection (*Re* = 0) were solved. The pure conduction numerical solution yields the exact value of conduction Nusselt number given by:

$$Nu_c = 2.0/ln\,(RR). \qquad (8)$$

3.1. Free convection

The numerical results of the average Nusselt number, *Nu* for free convection (*Re*=0) in a horizontal annulus is shown in fig. 2 for air (*Pr* = 0.71) in the range $1.20 \le RR \le 10$ and $0 \le Ra \le 10^6$. For the pure conduction regime (*Ra*=0), the average Nusselt number continuously decreases with the increase in *RR* as given in eq. (8). As *Ra* increases ($Ra \ge 10^2$), *Nu* first decreases with increasing *RR* which indicates the dominant conduction regime and then starts to increase with increasing RR when the flow changes to the laminar boundary layer regime. The value of *RR* at

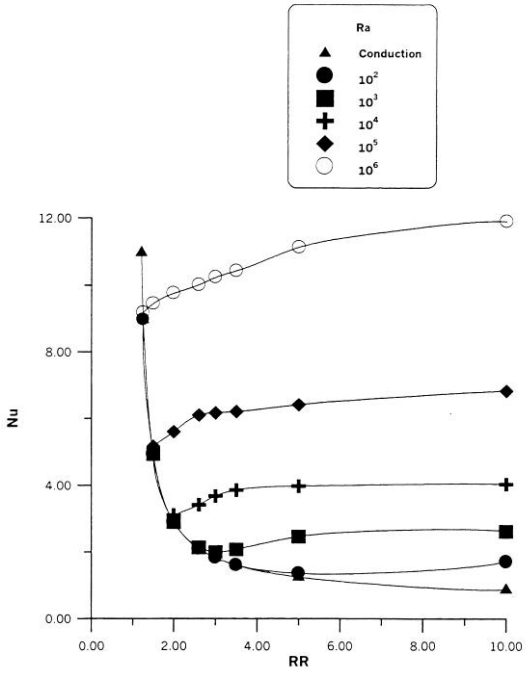

Fig. 2. Free convection in annular horizontal air layers (Pr = 0.71, Re = 0).

which the flow changes from pure conduction to laminar flow regime tends to be lower as Ra was increased. It is shown in the figure that increasing RR beyond the value of 5 has a little effect on Nu for $Ra \leq 10^5$. This shows that an annular space with $RR \geq 10$ behaves as if the inner hot cylinder was left alone as a single cylinder in a large medium of the fluid for $Ra \leq 10^5$. For higher Ra ($Ra > 10^5$), the radius ratio has to be increased much over 10 before we can consider the annular space as a single cylinder.

3.2. Inner rotating cylinder

The flow and heat transfer characteristics in a horizontal annulus with inner heated rotating cylinder and fixed outer cooled one are shown in figs. 3-6. Streamlines and isotherms are generated for RR = 2.6 and 5 for low and high Ra and different values of Re. Fig. 3 for RR = 2.6 and Ra = 100 shows the streamlines for free convection (Re = 0) as two crescent-shaped eddies as shown before in [2-4]. As Re increases ($Re \geq 100$), the eddies join together first at the top and gradually at the bottom to form circular cylinders. The isotherms for $Re \geq 0$ form concentric cylinders spaced regularly from the inner cylinder which indicates the pure conduction regime.

For $Ra = 10^6$ and Re = 0, fig. 4 shows the streamlines as two large eddies at the sides of the annulus. The size of the eddy on the right (inner cylinder rotating in the counter-clock wise direction) increases gradually with the increase in Re till it fills about 2/3 of the cavity at $Re = 10^3$. The isotherms indicate the boundary layer regime with large temperature changes at the cylinder walls. The isotherms are close to each other at the lower half of the inner cylinder which indicates higher local heat rates at these locations. As Re increases, the isotherms separate from the inner cylinder except at its bottom. This means lower heat transfer at higher Re.

To investigate the effect of RR on the flow, figs 5, 6 are given for RR = 5. The streamlines for Ra = 100 (fig. 5) show two eddies of the kidney-shape at Re = 0. As Re increases, the eddies form concentric cylinders till Re = 1000 where the concentric cylinders are distorted. The isotherms at Re = 0 form eccentric cylinders concentrated at the bottom of the inner cylinder which means high local Nu at the bottom. As Re increases, the isotherms become concentric cylinders indicating lower heat transfer. At Re = 1000, the isotherms turn to distorted cylinders near the inner cylinder.

For $Ra = 10^6$ and Re = 0, fig. 6 shows the streamlines as one small eddy on the right and a larger one on the left. As Re increases, the eddy on the right continuously gets bigger and the one on the left moves down closer to the bottom of the annulus. Small disturbances are shown at Re = 1000. The isotherms indicate the boundary layer regime with local Nu numbers at the inner cylinder higher than those at the outer one. It is noticed that the minimum local Nu number at the top of the inner cylinder moves to a location of higher φ as Re was increased.

The numerical values of Nu are plotted in figs. 7, 8 versus Ra for different values of Re and RR. For RR = 2.6, fig. 7 shows that increasing Re decreases Nu for $10^3 < Ra < 10^7$. For $Ra \leq 10^3$, pure conduction prevails and for $Ra \geq 10^7$ ($Gr/Re^2 > 1$), the effect of Re diminishes. The same behavior is shown in fig. 8 for

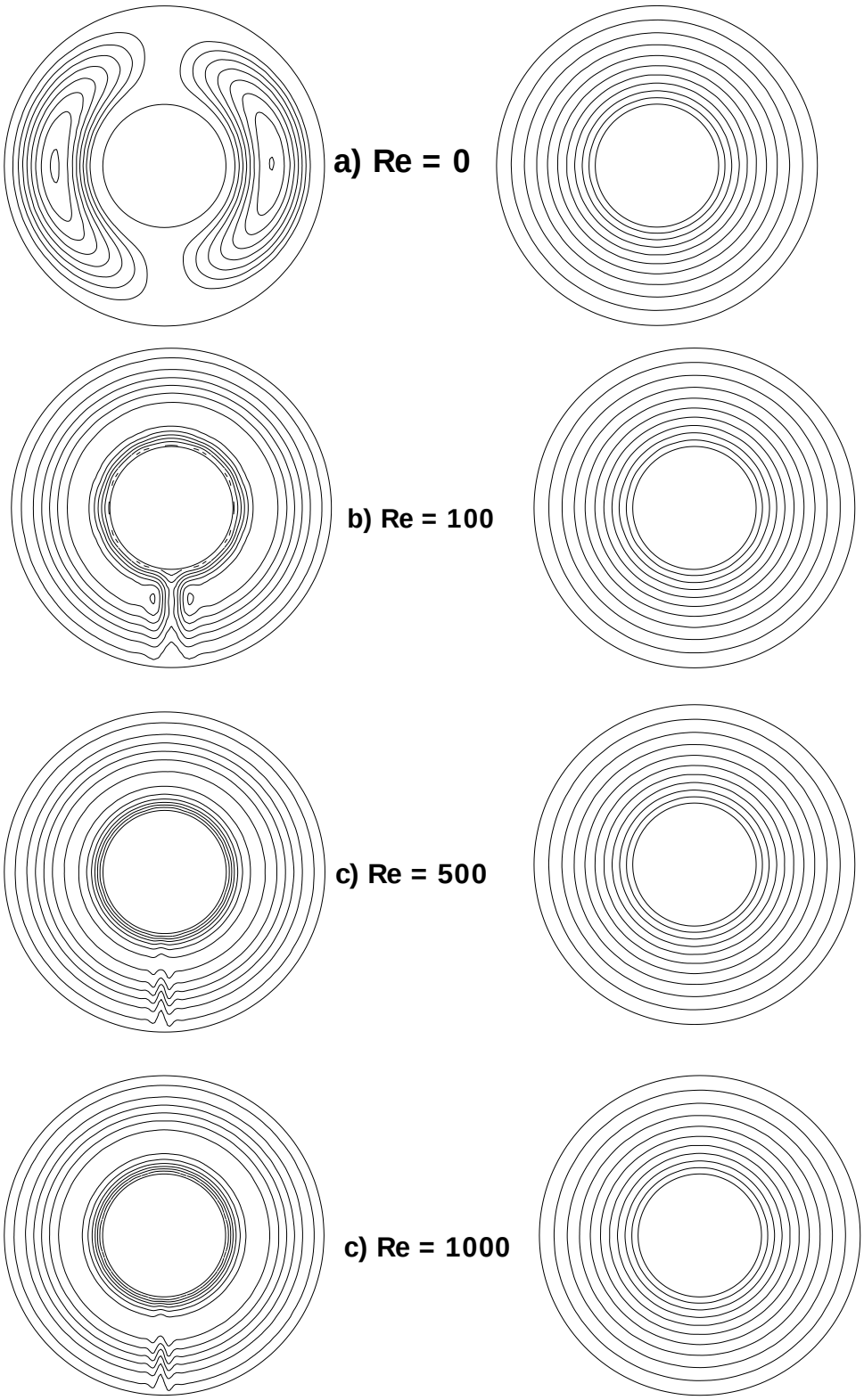

Fig. 3. Streamlines (left) and Isotherms (right) for air at $RR = 2.6$, and $Ra = 10^2$ (inner rotating cylinder).

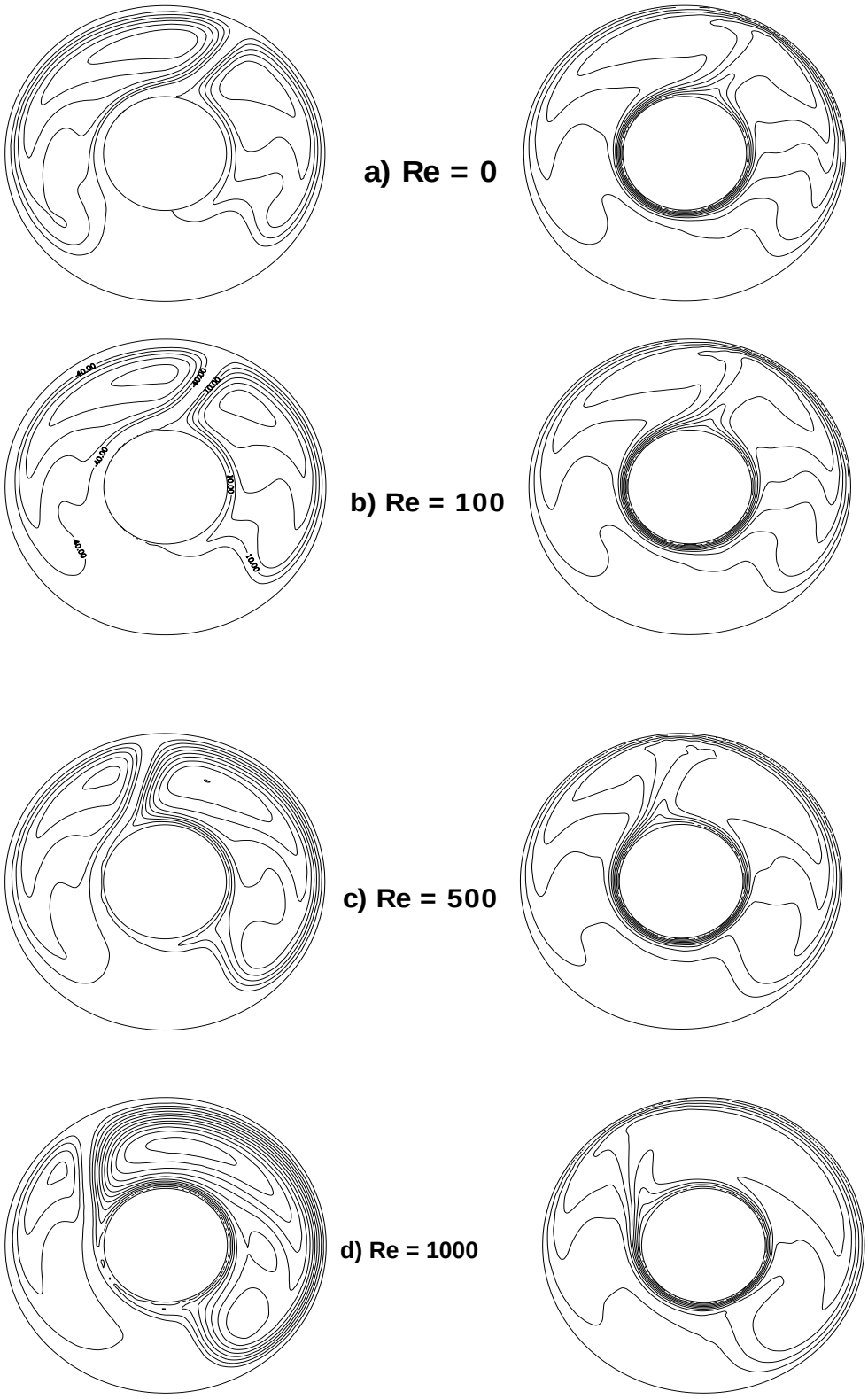

Fig. 4. Streamlines (left) and Isotherms (right) for air at $RR = 2.6$, and $Ra = 10^6$ (inner rotating cylinder).

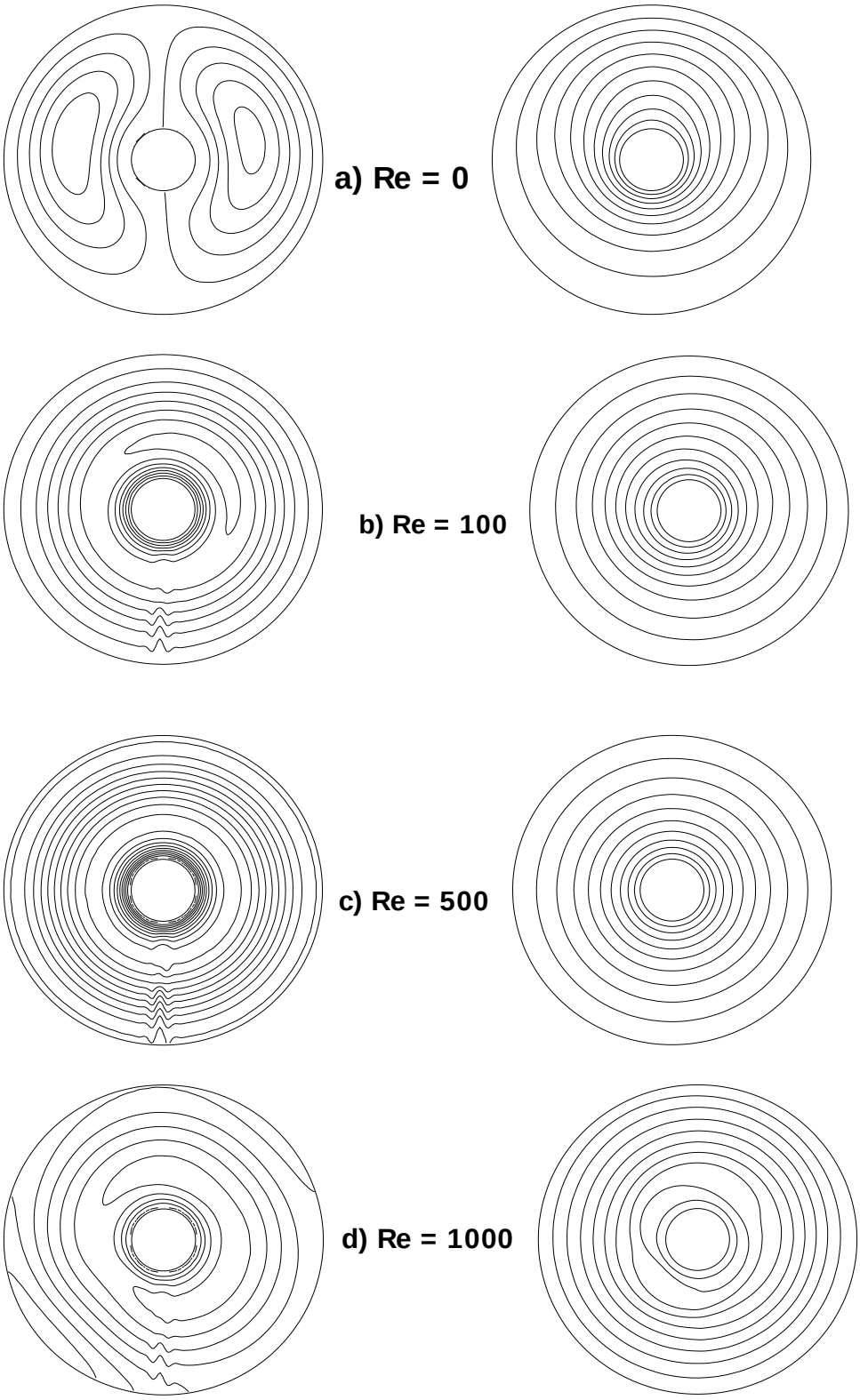

Fig. 5. Streamlines (left) and Isotherms (right) for air at $RR = 5$, and $Ra = 10^2$ (inner rotating cylinder).

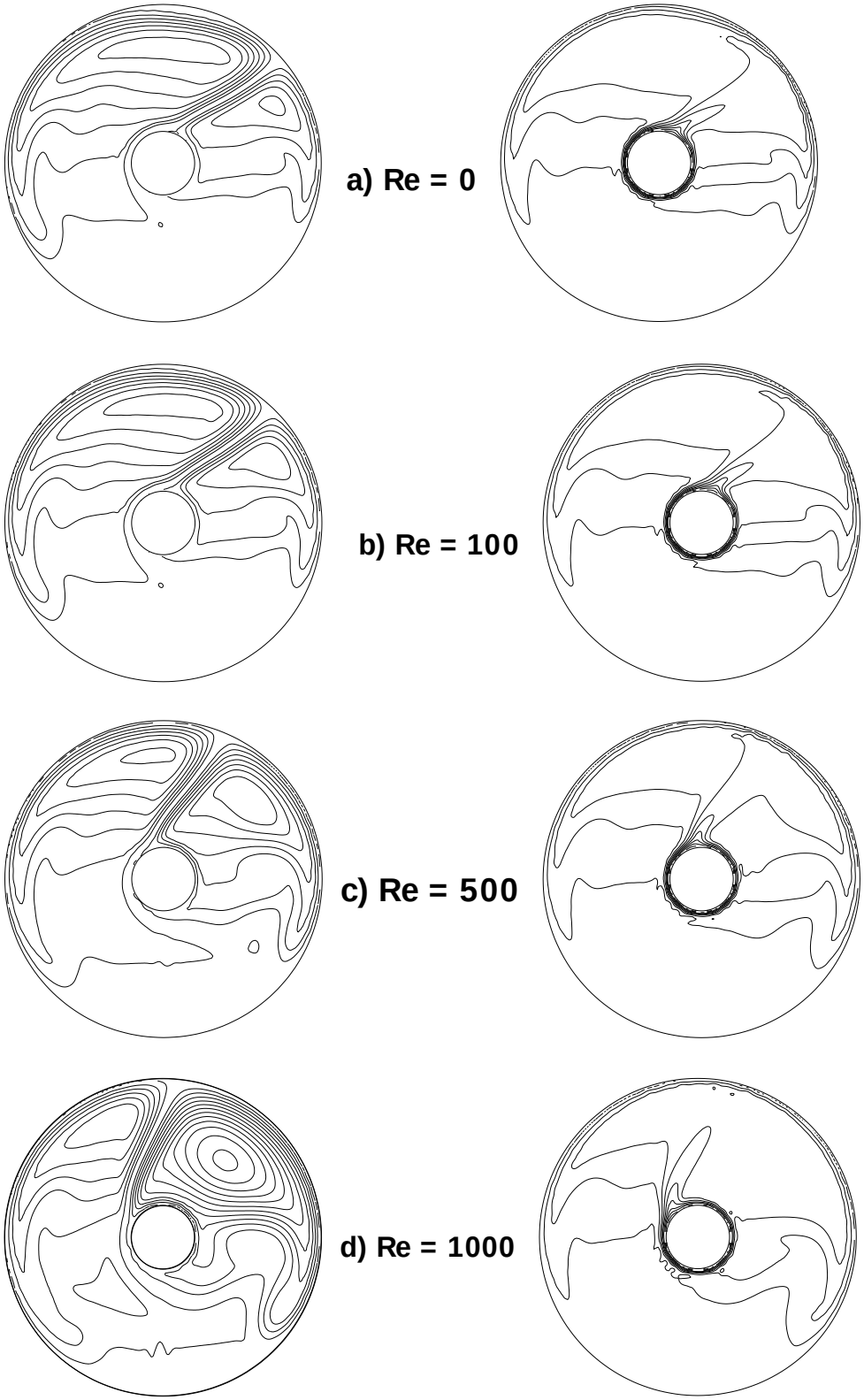

Fig. 6. Streamlines (left) and Isotherms (right) for air at $RR = 5$, and $Ra = 10^6$ (inner rotating cylinder).

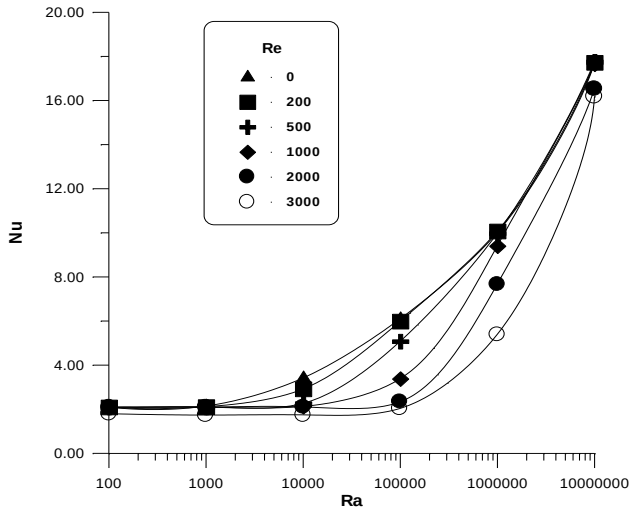

Fig. 7. Effects of *Ra* and *Re* on *Nu* for inner rotating cylinder (*Pr* = 0.71, *RR* = 2.6).

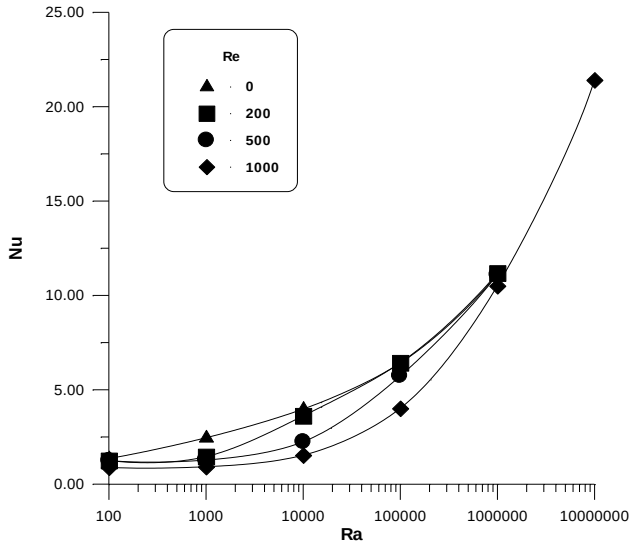

Fig. 8. Effects of *Ra* and *Re* on *Nu* for inner rotating cylinder (*Pr* = 0.71, *RR* = 5).

RR = 5. However, the effect of *Re* disappears at $Ra \geq 10^6$ ($Gr/Re^2 > 1$).

3.3. Outer rotating cylinder

In this case, the inner heated cylinder is fixed and the outer cooled one is rotating in the counter-clock wise direction. Fig. 9 shows the streamlines and isotherms for *RR* = 2 and *Ra* = 100. For free convection (*Re* = 0), the streamlines are shown as two crescent-shaped eddies. As *Re* was increased (*Re*≥200), the streamlines joined together forming concentric cylinders as in the case of inner rotating cylinder. The isotherms, for all Re, form concentric cylinders which assures the pure conduction regime. For $Ra = 10^5$, the case of free convection shows one big eddy on the left and another one on the right (fig. 10). As *Re* was increased (*Re*≥200), the size of the eddy on the left increased and finally joined the other one forming concentric cylinders except in the bottom. The isotherms for Re = 0 show the laminar boundary layer type of flow with higher local Nusselt number at the bottom of the inner cylinder. As *Re* was increased (*Re*≥200), the isotherms gradually changed to concentric cylinders and the convective flow was suppressed with a continuous reduction in the heat transfer till it reached the conduction limit at $Re = 10^3$.

For *RR* = 5 and *Ra* = 100, the isotherms, as shown in fig. 11, started at *Re* =0 as two kidney-shaped eddies and turned to concentric cylinders for *Re*≥200. The isotherms for *Re* = 0 are in the form of eccentric cylinders, indicating a slight increase in *Nu* over the pure conduction case. For higher *Re* (*Re*≥200), the isotherms form concentric cylinders which shows pure conduction regime. For $Ra = 10^5$, as shown in fig. 12, the streamlines start as two big eddies at *Re* = 0 and gradually merge together forming eccentric cylinders for *Re*≥200. The isotherms are concentrated around most of the inner cylinder showing a boundary layer type of flow at *Re* = 0. They gradually changed to eccentric cylinders for *Re*≥200 indicating a continuous reduction in *Nu*.

The effects of *Ra* and *Re* on *Nu* are shown in figs. 13, 14 for *RR* = 2 and 5. For *RR* = 2, fig. 13 shows that the pure conduction regime prevails up to $Ra = 10^4$ for all values of *Re*. For $10^4 < Ra < 10^7$, increasing *Re* from 0 to 1000 decreased the average Nusselt number. For *RR* = 5, a similar behavior was shown in fig. 14. However, the laminar convection boundary layer regime started earlier at $Ra = 10^2$. Increasing *Re* has the significant effect of suppressing the convection flow and decreasing the average Nusselt number.

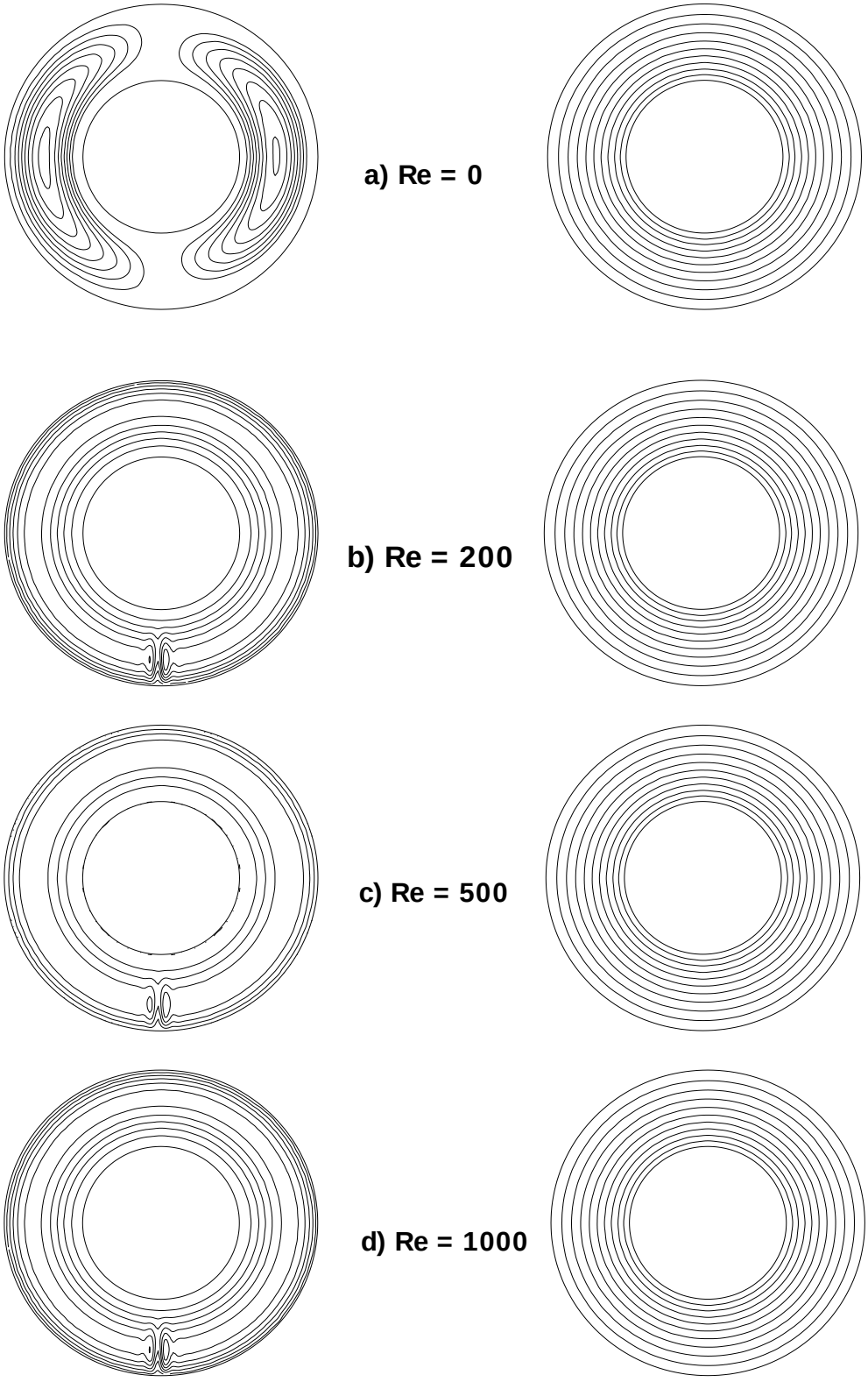

Fig. 9. Streamlines (left) and isotherms (right) for air at $RR = 2$ and $Ra = 100$ (outer rotating cylinder).

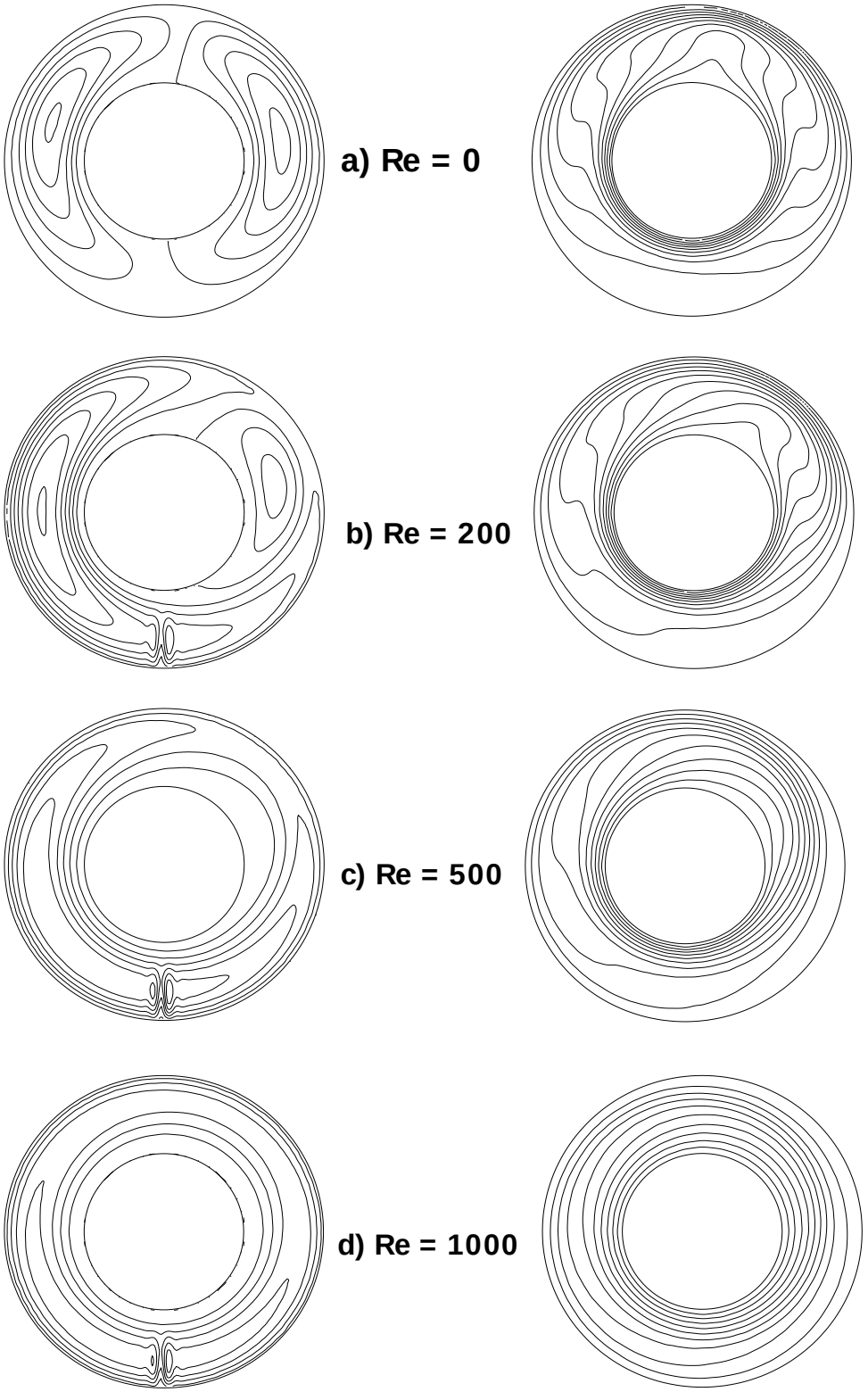

Fig. 10. Streamlines (left) and isotherms (right) for air at $RR = 2$ and $Ra = 10^5$ (outer rotating cylinder).

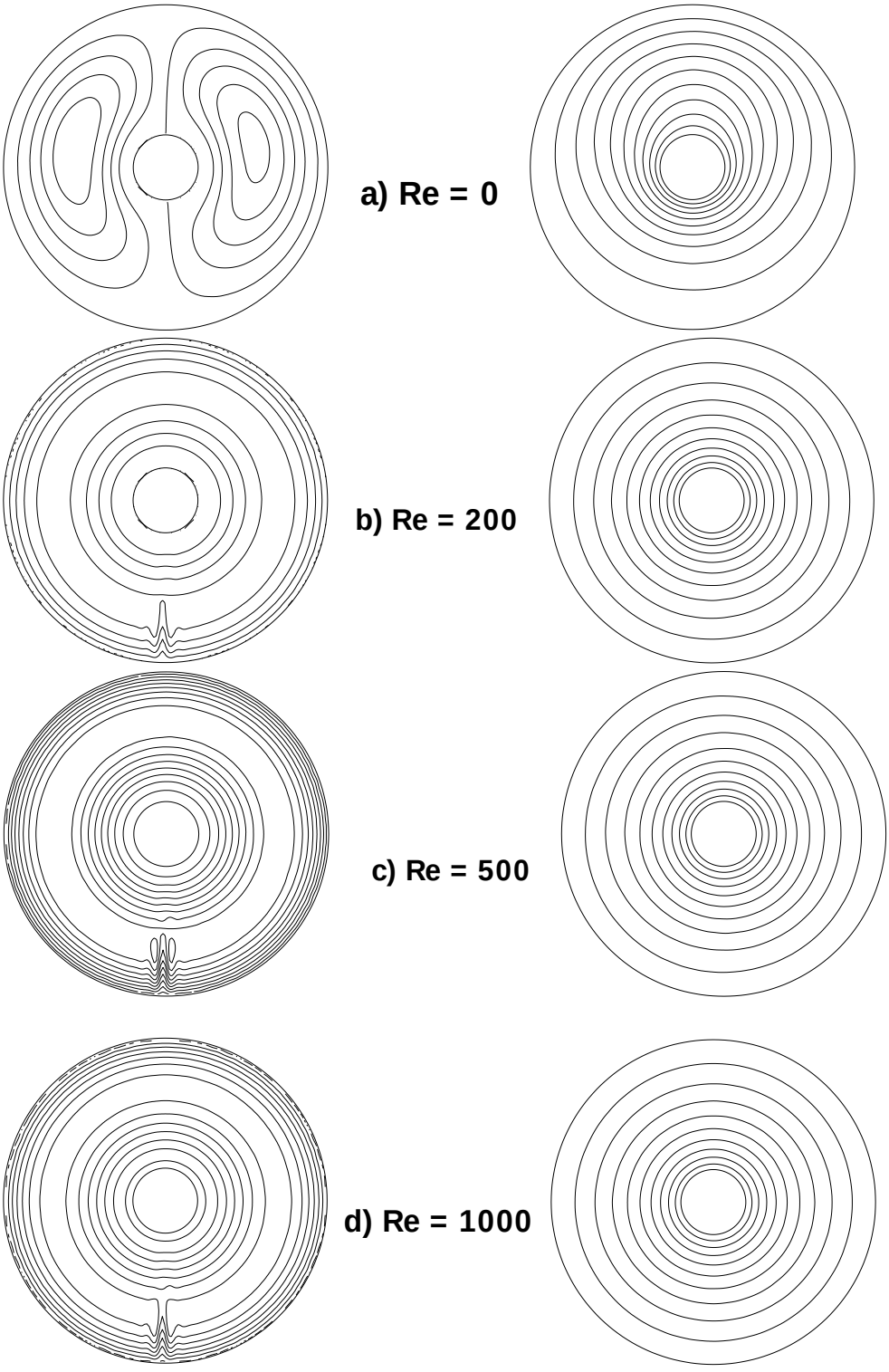

Fig. 11. Streamlines (left) and isotherms (right) for air at *RR* = 5 and *Ra* = 100 (outer rotating cylinder).

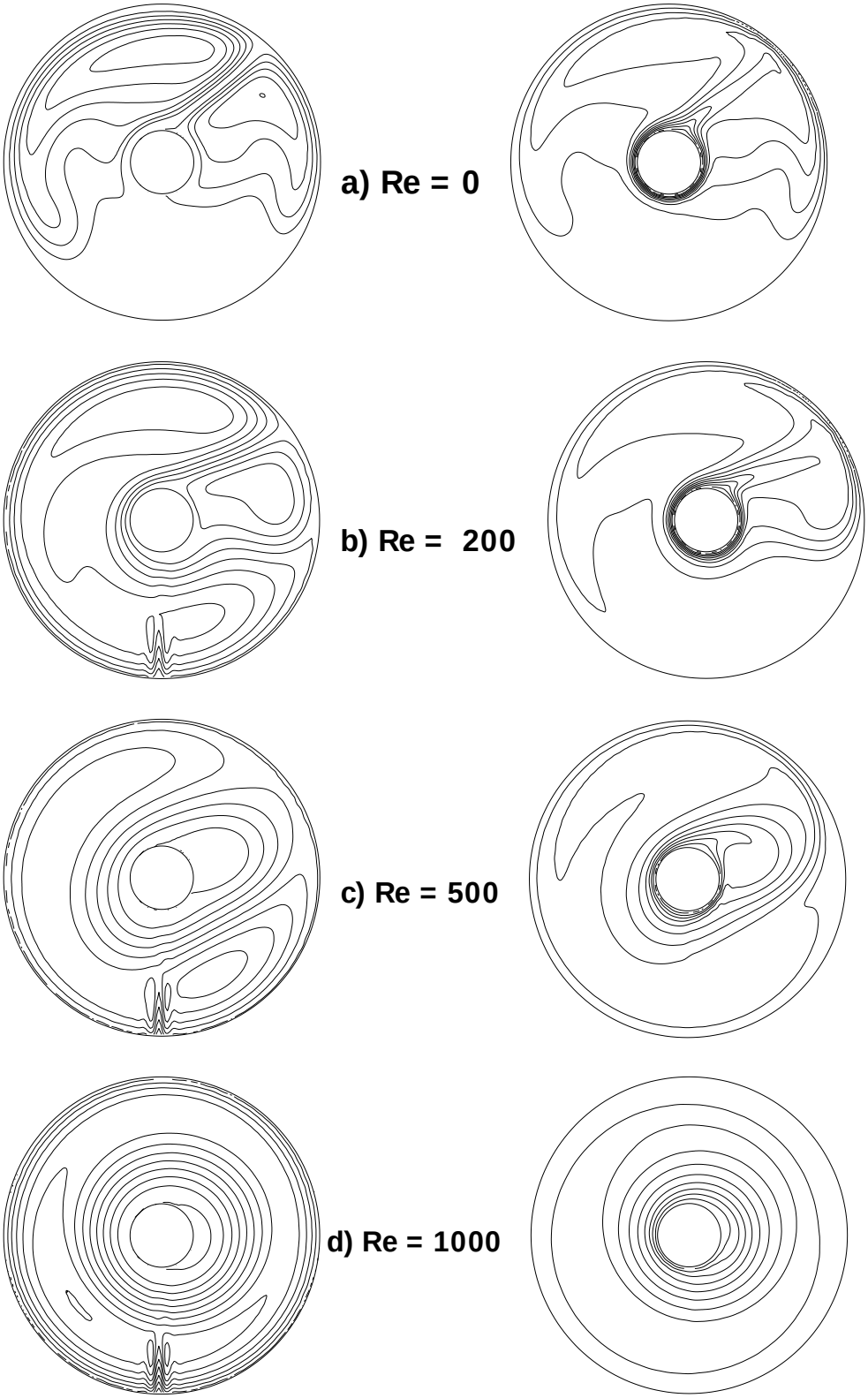

Fig.12. Streamlines (left) and isotherms (right) for air at $RR = 5$ and $Ra = 10^5$ (outer rotating cylinder).

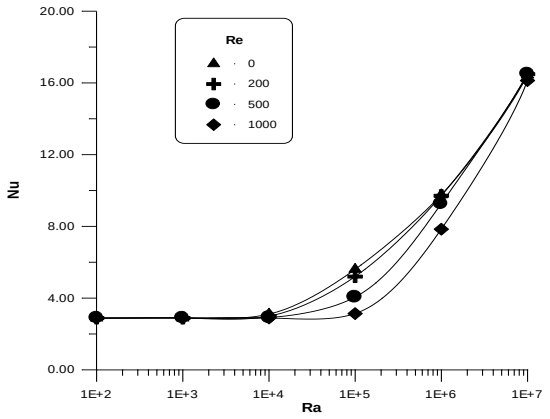

Fig. 13. Effects of *Ra* and *Re* on *Nu* for outer rotating cylinder (*Pr* = 0.71, *RR* = 2).

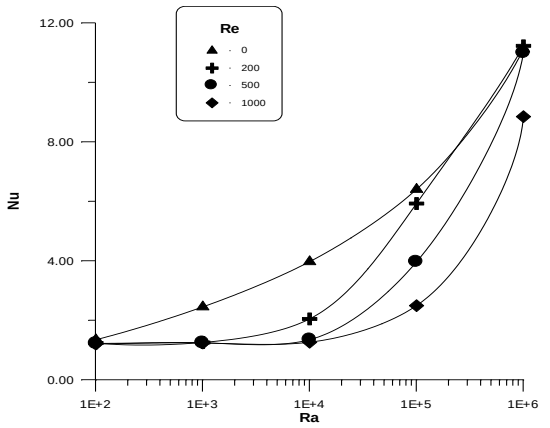

Fig. 14. Effects of *Ra* and *Re* on *Nu* for outer rotating cylinder (*Pr* = 0.71, *RR* = 5).

4. Conclusions

The laminar mixed convective heat transfer in horizontal air layers between two concentric infinite cylinders at different uniform temperatures is numerically solved. For free convection at $Ra \le 10^5$, the annulus simulates a single cylinder if $RR \ge 10$. For $Ra > 10^5$, *RR* should be taken much higher than 10. For mixed convection, the convective flow started earlier as the radius ratio was increased. The effect of *Re* was to suppress the convective flow as *Re* was increased. For $Gr / Re^2 > 1$, the effect of *Re* on the average heat transfer is greatly reduced. Under the same circumstances, the inner rotating cylinder gives slightly higher heat transfer than that for outer rotating cylinder.

Nomenclature

a is the radius of inner hot cylinder, ($a = r_i$), m,
c_p is the specific heat, J/kgK,
g is the gravitational acceleration, m/s^2,
Gr is the Grashof number, $g\beta(T_h - T_c)(2a)^3/\nu^2$.
h is the average heat transfer coefficient, W/m^{2}K,
h_ϕ is the local heat transfer coefficient , W/m^{2}K,
k is the thermal conductivity, W/mK,
Nu is the average Nusselt number, $h(2a)/k$,
Nu_c is the conduction Nusselt number
Nu_ϕ is the local Nusselt number, $h_\phi(2a)/$k,
p_d is the dynamic pressure, N/m^2,
P_d is the dimensionless dynamic pressure, $P_d = \dfrac{p_d}{\rho(\nu/a)^2}$
Pr is the Prandtl number, $\mu c_p/$k,
r is the radial coordinate, m,
r_i is the radius of inner cylinder, m,
r_o is the radius of outer cylinder, m,
R is the dimensionless radial coordinate, r/a,
Ra is the Rayleigh number, $g\beta(T_h - T_c)(2a)^3/\nu\alpha$,
Re is the Reynolds number, $(\omega a).2a/\ \nu$,
RR is the radius ratio, r_0/r_i ,
T is the local fluid temperature, K,
υ_r is the radial velocity, m/s,
V_r is the dimensionless radial velocity, $V_r = \upsilon_r/(\nu/a)$,
υ_ϕ is the angular velocity, m/s, and
V_ϕ is the dimensionless angular velocity, $V_\varphi = \upsilon_\varphi/(\nu/a)$.

Greek

α is the thermal diffusivity, $k/c_p\rho$, m^2/s,
β is the coefficient of volumetric thermal expansion, K^{-1},
θ is the dimensionless temperature, $(T-T_c)/(T_h-T_c)$,
μ is the dynamic viscosity, kg/ms,
ν is the kinematic viscosity, μ/ρ, m^2/s
ρ is the local density, kg/m^3,
ϕ is the angular coordinate, rad , and
ω is the angular velocity, rad/s.

Subscripts

c is the cold,
h is the hot,
i is the inner, and
o is the outer.

References

[1] T.H. Kuehn and R.J. Goldstein, "An Experimental And Theoretical Study of Natural Convection in the Annulus Between Horizontal Concentric Cylinders", J. Fluid Mech., Vol. 74 (4), pp. 695-719 (1976).

[2] R.E. Powe, C.T. Carley and E.H. Bishop, "Free Convective Flow Patterns in Cylindrical Annuli", J. Heat Transfer, Vol. 91, pp. 310-314 (1969).

[3] R.E. Powe, C.T. Carley and S.L. Carruth, "A Numerical Solution for Natural Convection in Cylindrical Annuli", J. Heat Transfer, Vol. 93, pp. 210-220 (1971).

[4] Y.F. Rao, Y. Miki, K. Fukuda, Y. Takata and S. Hasegawa, "Flow Patterns of Natural Convection in Horizontal Cylindrical Annuli", Int. J. Heat Mass Transfer, Vol. 28 (3), pp. 705-714 (1985).

[5] J.S Yoo, "Dual Steady Solutions in Natural Convection Between Horizontal concentric Cylinders", Int. J. Heat Mass Transfer, Vol. 17, pp. 587-593 (1996).

[6] C.H. Cho, K.S. Chang and K.H. Park, "Numerical Simulation of Natural Convection in Concentric and Eccentric Horizontal Cylindrical Annuli", J. Heat Transfer, Vol. 104, pp. 624-630 (1982).

[7] Y.Z. Wang and H.H. Bau, "Low Rayleigh Number Convection in Horizontal Eccentric Annuli", ASME Winter Annual Meeting, Chicago, Illinois, HTD-Vol. 99 (1988).

[8] Z.Y Guo and Zhang, " Thermal Drive in Centrifugal Fields-Mixed Convection in a Vertical Rotating Cylinder", Int. J. Heat Mass Transfer, Vol. 35, pp. 1635-1644 (1992).

[9] M.A.I. El-Shaarawi and M. Khamis, "Induced Flow in Uniformly Heated Vertical Annuli With Rotating Inner Walls", Numerical Heat Transfer, Vol. 12, pp. 493-508 (1987).

[10] M.A. Hessami, G.D.V. Davis, E. Lenonardi and J.A. Reizes, "Mixed Convection in vertical cylinder annuli", Int. J. Heat Mass Transfer, Vol. 30, pp. 151-164 (1987).

[11] T. Fusegi, B. Farouk and K.S. Ball, "Mixed-Convection Flows Within a Horizontal Concentric Annulus With a Heated Rotating Inner Cylinder", Numerical Heat Transfer, Vol. 9, pp. 591-604 (1986).

[12] T.S. Lee, "Laminar Fluid Convection Between Concentric and Eccentric Heated Horizontal Rotating Cylinders for low Prandtl Number Fluids", Int. J. Numerical Methods in Fluids, Vol. 14, pp. 1037-1062 (1992).

[13] T.S. Lee, "Numerical Computation of Fluid Convection With air Enclosed Between the Annuli of Eccentric Heated Horizontal Rotating Cylinders", Computers and Fluids, Vol. 21, pp. 355-368 (1992).

[14] T.S. Lee, "Numerical Experiments with Laminar Fluid Convection Between Concentric and Eccentric Heating Rotating Cylinders", Numerical Heat Transfer, Vol. 7, pp. 77-87 (1984).

[15] G.I. Taylor, "Stability of a Viscous Liquid Contained Between two Rotating Cylinders", Philosophical Transactions, Royal Society (London), Series A, Vol. 223, p. 289 (1923).

[16] I.S. Bjorklund and W.M. Kays, "Heat Transfer Between Concentric Rotating Cylinders", J. Heat Transfer, Vol. 81, pp. 175-186 (1959).

[17] R.C. DiPrima and H.L. Swinney, "Instabilities and Transition in Flow Between Concentric Rotating Cylinders," In Topics in applied physics., Vol. 45, ed. H.L. Swinney and J.P. Gollub, Springer, Berlin, pp.139-180 (1981).

[18] J.S Yoo, "Mixed Convection of Air Between Two Horizontal Concentric Cylinders with a Cooled Rotating Outer Cylinder", Int. J. Heat Mass Transfer, Vol. 41, pp. 293-302 (1998).

[19] S. V. Patankar, Numerical Heat Transfer and Fluid Flow, Mc Graw-Hill, New York (1980).

Received July 26, 2004
Accepted September 9, 2004